Published by IOP Publishing for Sissa Medialab

Received: *January 16, 2025*
Revised: *March 15, 2026*
Accepted: *April 10, 2026*
Published: *May 5, 2026*

8th International Conference on Micro Pattern Gaseous Detectors
University of Science and Technology of China, Hefei, China
14–18 October 2024

2026 JINST 21 C05004

Investigation of a Time Projection Chamber with high granularity readout for the circular e^+e^- collider

J.B. Zheng,[a,b,c] **H.R. Qi**[a,b,c,*] **J.X. Zhang,**[a,b,c] **X. She**[a,b,c] **and H.Y. Mao**[d]

[a] *University of Chinese Academy of Sciences,*
No. 1 Yanqihu East Road, Beijing, China
[b] *Institute of High Energy Physics, CAS,*
No. 19 Yuquan Road, Shijingshan District, Beijing, China
[c] *State Key Laboratory of Particle Detection and Electronics,*
No. 19 Yuquan Road, Shijingshan District, Beijing, China
[d] *National University of Singapore,*
21 Lower Kent Ridge Road, Singapore, Singapore

E-mail: qihr@ihep.ac.cn

Abstract: Future e^+e^- collider projects, such as the International Linear Collider (ILC), the Circular Electron Positron Collider (CEPC), and the Future Circular Collider (FCC-ee), require the development of high performance main tracking detectors. Time Projection Chambers represent an attractive option for large-volume tracking systems in these experiments. To meet the demanding physics requirements, the detector concept foresees a large scale three dimensional tracking system based on a TPC operating in a 3.0 T solenoidal magnetic field, with a target spatial resolution of about 100 µm. The detector must also achieve a longitudinal position resolution of a few hundred micrometers while providing excellent particle identification (PID) performance with a resolution better than 3%. To address these requirements, a high granularity readout TPC technology has been developed. The feasibility of this approach for the CEPC has been investigated through detailed simulations, including studies at the low luminosity Z operation. The critical detector performance such as spatial resolution, drift velocity, and PID efficiency through cluster counting has been systematically evaluated. Compared with the conventional large pad readout, TPC detector with the high granularity readout delivers the good spatial resolution, high tracking efficiency and robust PID capabilities.

Keywords: Gaseous detectors; Time projection Chambers (TPC); dE/dx detectors

*Corresponding author.

https://doi.org/10.1088/1748-0221/21/05/C05004

Contents

2026 JINST 21 C05004

1 Introduction

The Time Projection Chamber (TPC) concept comprises a large chamber filled with a suitable gas mixture, within which a uniform electric field of several hundred V/cm is established parallel to the magnetic field of CEPC detector concept. As charged particles traverse the gas, they ionize the gas molecules, releasing electrons that drift toward an endplate of the TPC. These electrons undergo gas amplification at the endplate and are spatially sampled via a segmented anode of the different size readout, which allows the estimation of track-segment coordinates in the plane parallel to the endplate and time-based coordinate reconstruction along the drift direction. The TPC has been widely adopted in high-energy physics experiments due to its low material budget and excellent pattern recognition capability, rendering it an ideal choice for three-dimensional tracking and identification of charged particles. In environments with high particle rates and intense background noise, the TPC must achieve efficient positive-ion suppression and support track correction integrated with the outer silicon detectors. As a result, TPCs are predominantly employed as tracking detectors in collider experiments. However, the detection precision of current TPCs can no longer meet the stringent requirements of future particle physics experiments, such as ILC [1] and the CEPC [2]. These experiments demand further performance enhancements of the TPC. The TPC investigated in this paper is the first verification prototype designed in accordance with the requirements of next-generation particle physics experiments. Its design complies with the specifications for the CEPC, as detailed in table 1. The overall parameters of the TPC detector are presented in the table, with special emphasis on the detector readout module. This study adopts a readout module design that conforms to these specifications. Employing a TPC as the main tracking detector in a circular collider experiment offers several distinct advantages: particle tracks can be reconstructed using a large number of three-dimensional (r, ϕ, z) spatial points, and the moderate point resolution and double-hit resolution (in comparison with silicon detectors) are effectively compensated for by continuous tracking.

A schematic diagram of TPC is shown in figure 1. The TPC is designed as a large cylindrical structure with an outer diameter of 3.6 m and an overall length of approximately 5.9 m. The ultra-light composite inner and outer cylindrical walls with a low material budget, equipped with field-forming strips connected to a resistor divider network, serve to maintain the uniform electric field in the chamber. A central cathode, which partitions the TPC into two independent drift volumes, is biased at approximately -62 kV, while the endplates and other outer surfaces of the TPC are electrically grounded. Consequently, the composite walls must be capable of withstanding the high electric

Table 1. Key parameters of TPC tracker in CEPC detector concept.

TPC detector	Key Parameters
Modules per endplate	248 modules/endplate
Geometry of layout	Inner: 1.2 m Outer: 3.6 m Length: 5.9 m
Potential at cathode	-62,000 V
Gas mixture	T2K: Ar/CF_4/iC_4H_{10}=95/3/2
Maximum drift time	34 µs @ 2.75 m
Detector modules	High granularity readout Micromegas

potential of the central cathode. To maintain a uniform electric field within the active TPC volume, a narrow strip pitch with mirror strip structures is employed; this configuration forms the electrodes of the field cage, which precisely shapes the electric field distribution in the detection volume.

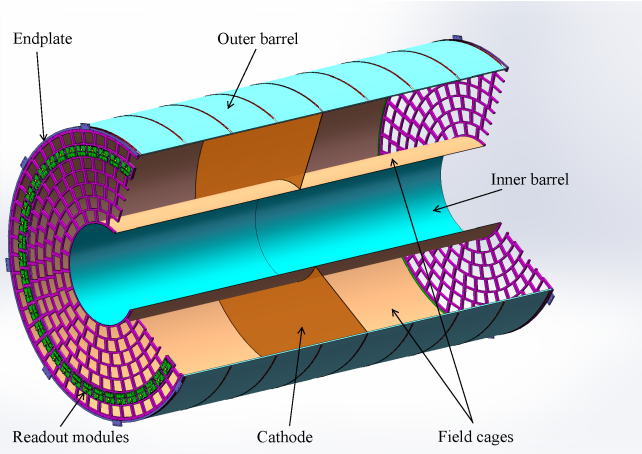

Figure 1. Layout of the high granularity readout TPC, which is a cylindrical, gas-filled tracking detector aligned with the beam axis, comprising a barrel and two end-plates.

2 Simulation and performance

2.1 Simulation and digitization framework

Given the substantial size of the TPC, its extended drift path of over 2.7 m, and the intricate physical processes involved in its design, performing comprehensive simulations with Garfield++ would incur substantial computational resource costs and excessive processing time. In this context, the iterative adjustment and optimization of detector parameters pose an extremely arduous challenge. Consequently, a parametrised simulation framework was developed to model the complex simulation process, significantly reducing the required computational resources. Detailed simulation and digitization workflows are delineated in figure 2. Ionization data of charged particles are generated directly via the Garfield++ track-Heed interface, whereas the processes of electron diffusion and multiplication are modelled parametrically rather than simulated directly. Positional, energetic, and temporal data of the ionization-induced clusters and electrons are recorded in the Monte Carlo (MC) truth for subsequent application in the drift and multiplication parametric models. Electrons that have

2026 JINST 21 C05004

undergone gas amplification are collected by the readout structure. Parameters for simulating electronic noise are derived from Application-Specific Integrated Circuit (ASIC) testing and implemented as a parameterized noise model that is applied in the digitization stage.

This information is stored in the MC truth and utilized for subsequent simulation processes within the software framework. The MC truth is essential for the investigation of primary ionization clusters, as it provides the spatial distribution of these clusters and the corresponding number of electrons per cluster. A simulation of 20 GeV pion ionization in the T2K gas mixture was conducted over a 1.2 m path to generate primary ionization clusters, which serve as input for the workflow illustrated in figure 2. The distribution of ionization electrons generated by a 20 GeV π particle following 50 cm of drift and amplification by a Micromegas detector, as derived from Garfield++ simulations is presented in the top right panel of figure 2. Following gas amplification and diffusion, the electron cloud forms discrete clusters with inhomogeneous charge densities, a distribution characteristic that is consistent with the Polya distribution.

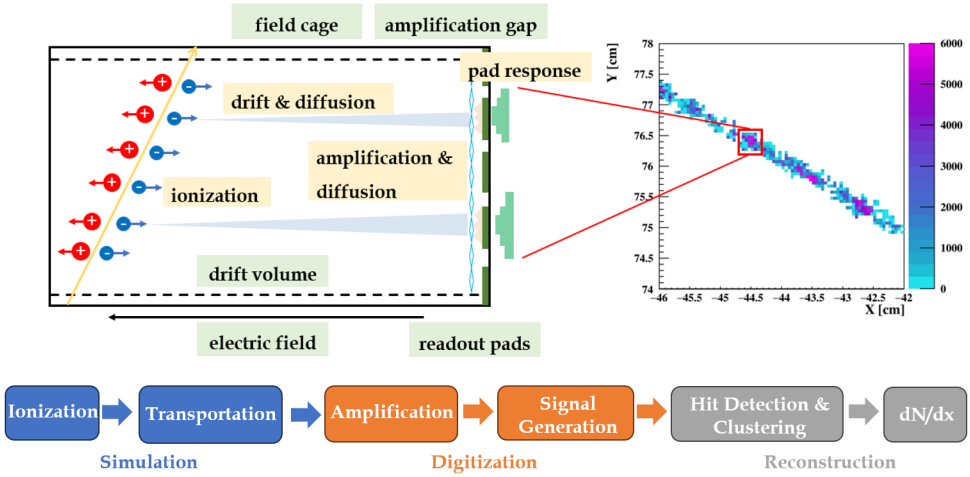

Figure 2. Workflow of TPC simulation and digitization (the incident angle is defined as $\theta = 90°$ when the particle track is perpendicular).

A simulation was conducted to evaluate the number of initial ionization clusters per centimeter for π and K particles in the T2K gas mixture as a function of particle momentum. The results reveal a significant difference in the number of initial ionization clusters generated by π and K particles at the same momentum in the T2K gas mixture, with the exception of the region near the minimum ionizing particle point. Specifically, π particles produce a greater number of clusters than K particles, with the magnitude of this difference dependent on the particle momentum. These results are consistent with theoretical expectations based on the Bethe-Bloch formula, which describes the dependence of dE/dx on particle velocity. These detailed simulations of ionization and electron cloud formation provide the foundational basis for PID performance studies presented in the following section.

2.2 Spatial resolution

In the TPC detector, spatial resolution is primarily limited by the diffusion effect induced by the long-distance drift of ionization electrons. Figure 3 shows the comparison of transverse spatial resolution as a function of drift distance under different operating conditions. The curves are calculated

2026 JINST 21 C05004

using equation (2.1), where $\sigma^{\text{pad}}_{r\phi_0}$ denotes the geometric intrinsic resolution, $D_{r\phi}$ is the transverse diffusion coefficient of the gas mixture, and L represents the drift distance. The red curve corresponds to the transverse spatial resolution of the high-granularity readout mode (single-electron readout), while the magenta curve represents that of the 1 mm × 6 mm pad readout mode. An indirect comparison between the traditional pad readout and the 500 µm × 500 µm high-granularity readout can be achieved by clustering the small pads to match the same effective area, with the result presented as the green curve. The results demonstrate that the high-granularity readout mode achieves a superior spatial resolution compared to the pad readout mode.

$$\sigma^{\text{pad}}_{r\phi} = \sqrt{(\sigma^{\text{pad}}_{r\phi_0})^2 + LD^2_{r\phi}} \tag{2.1}$$

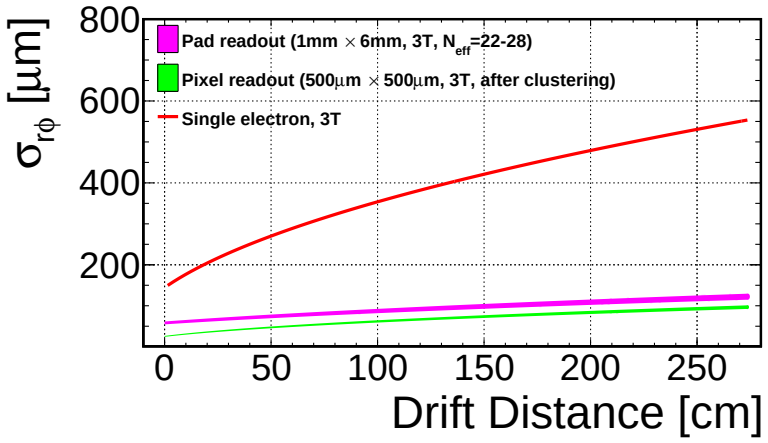

Figure 3. Spatial resolution as a function of the drift length for different configurations of the readout plane: 1 mm × 6 mm pads (solid magenta); 500 µm × 500 µm pads (single electron) (solid red); 500 µm × 500 µm pads after clustering (green solid).

2.3 Particle identification performance

PID performance is a critical parameter for the TPC's operational performance. The dE/dx method adopts a parallel processing structure, which calculates the total energy deposition per layer and takes the average of truncated data to estimate the energy loss per unit track length. The dn/dx method leverages the proportional relationship between ionization events and the Landau distribution in the number of activated pads across different TPC layers. In practice, the dn/dx method counts the number of threshold crossing pads, and the value of n is derived as the mean of the truncated sample, which represents the average number of threshold crossing pads along the track length. The simulation also assesses the impact of different readout unit sizes and incident angles ($\theta = 60°$ and $\theta = 85°$ within the chamber) on resolution performance, as illustrated in figure 4.

The results clearly demonstrate that the overall resolution of millimeter-scale pad-type readout units is inferior to that of the 500 µm × 500 µm pixelated readout units. The dE/dx resolution can be estimated using the empirical formula (2.2) [3]:

$$\frac{\sigma_{dE/dx}}{\langle dE/dx \rangle} \propto L^{-0.45} G^{-0.13} \tag{2.2}$$

2026 JINST 21 C05004

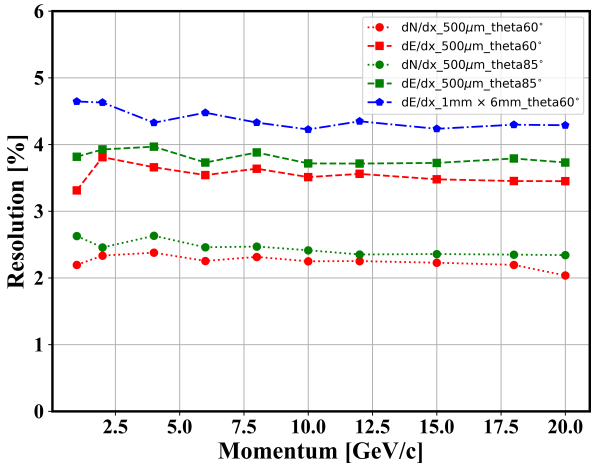

Figure 4. dE/dx resolution performance under various momenta, incident angles and readout sizes.

where L is the track length and G is the number of samples (e.g., pad rows). This formula is applicable to large-area readout pads (millimeter-scale) and traditional dE/dx measurement methods. For the high-granularity readout mode, a fully developed simulation framework must be employed instead. According to this relation, the expected resolution of the pad-type readout for a 138 cm track length is approximately 4.8%. This value corresponds to the expected ionization energy loss resolution of the large pad readout, while the pixelated readout units achieve significantly better performance, as illustrated in figure 4. It is evident from the equation that reducing the size of the readout pads contributes moderately to the improvement of dE/dx measurement accuracy. However, it is important to note that this reduction in readout pad size also introduces a more complex electronic interconnection system, which constitutes a necessary trade-off. Larger readout unit sizes result in the loss of fine details in particle information recording, thereby degrading the resolution performance. Thus, pixelated readout modes exhibit superior resolution performance relative to pad-type readout modes. Additionally, in contrast to PID performance, the resolution is nearly unaffected by particle momentum, with any minor fluctuations being primarily attributed to system optimization parameters. For $\theta = 60°$ and $\theta = 85°$, the shorter track lengths and longer drift distances slightly degrade the resolution to approximately 2.4%, a value that is still significantly superior to the 4.8% estimate derived from the empirical formula. The high granularity of the detector system increases the number of readout channels, while a higher level of electronic integration for the detector module further adds to the system complexity. Collectively, these two factors result in a higher overall power dissipation for the TPC system. To mitigate the excessive cooling requirements imposed by this elevated power dissipation, the TPC detector system is investigating low-power design strategies to reduce the power consumption of the front-end electronics. A dedicated prototype has therefore been developed to validate this low-power design concept.

3 High granularity readout TPC prototype R&D

A TEPIX ASIC prototype chip has been developed to demonstrate its design and performance [4]. Given the criticality of power consumption, this prototype adopts a 180 nm Complementary Metal Oxide Semiconductor (CMOS) process and a circuit architecture based on simple analog circuits to

2026 JINST 21 C05004

overcome these technical challenges. This chip integrates 128 channels and has a physical size of 2.2 mm × 5.6 mm. The test results of this prototype are presented in table 2. The noise and power consumption of the chip are higher than the designed specifications, and both performance metrics will be optimized by adopting an advanced 65 nm process in subsequent research work.

Table 2. Test results of the TEPIX chip using 180 nm.

Parameters	Test results	Design specifications
Number of channels	128	128
Equivalent Noise Charge	300 e^-	200 e^-
Dynamic range	25 fC	25 fC
Integral Non-linearity	<1%	<1%
Time resolution	10 ns	10 ns
Analog-to-Digital Converter	10 bits	10 bits
Total power consumption	0.3 mW/ch	0.15 mW/ch

In the experimental tests, the master bias current of the Analog Front-End (AFE) can be adjusted via an external resistor. The total current drawn by the test PCB increases linearly with the master bias current. To estimate the power consumption of the AFE, we postulated a linear proportionality between the AFE operating current and the master bias current. Therefore, the quiescent current consumed by all other components on the PCB can be derived from the y-intercept of the linear fit, which was measured to be 9.73 mA. Based on this derivation, the power consumption of the AFE was estimated to be 2.0 mW per channel at a nominal master bias current of 25 µA, a value that is in good agreement with the corresponding simulation result of 3.0 mW. Test results for the AFE and the Successive Approximation Register Analog-to-Digital Converter (SAR ADC) exhibit excellent agreement with the predefined performance metrics, thus meeting the required performance specifications. The power consumption of the full AFE and ADC core circuit set has been optimized to approximately 3.0 mW per channel, corresponding to a significant reduction of at least 50% relative to other state-of-the-art ASICs with analogous architectural designs.

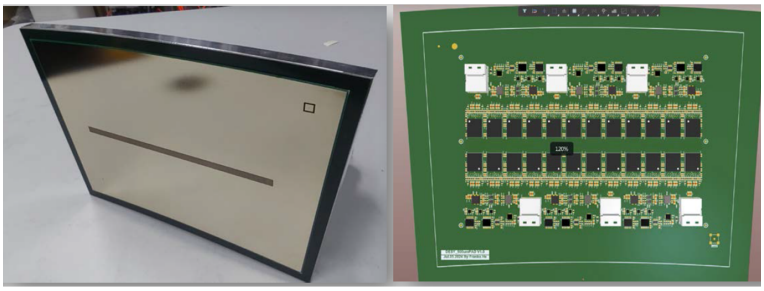

Figure 5. Prototype of the high granularity readout TPC detector module integrated with the Front-End Electronics readout chips.

The Micro Pattern Gaseous Detector (MPGD) — a class of gaseous detectors exemplified by Micromegas — possesses inherent advantages, as its intrinsic electric field configuration functions naturally as a transmission gate for electron transport and a blocking layer for ion backflow (IBF). Adding an additional mesh can further enhance the IBF suppression capability of Micromegas detectors.

2026 JINST 21 C05004

Double-mesh Micromegas detectors have been studied by the group at the University of Science and Technology of China (USTC) [5]. At a gain of about 2000, the product IBF × gain can be reduced to below 1. In forthcoming measurements, positive-ion suppression will be implemented using double- or multi-layer mesh structures.

The design of the PCB board for a single detector module is detailed in the endplate design scheme, as illustrated in figure 5. Each detector module consists of individual readout units, each with a physical size of 500 µm × 500 µm and an inter-unit spacing of 100 µm. This high-density layout facilitates high-precision spatial resolution measurements via a fine-pitch readout pad array, as also illustrated in figure 5. In terms of the detector module design, the PCB board has dimensional specifications matching those of the aluminum alloy support frame, with an overall size of about 230 mm × 170 mm. To meet the installation requirements of the detector module, the PCB board adopts a curved-edge design and is fitted with two high-precision positioning holes. These structural features ensure accurate alignment and a secure mechanical connection between the PCB board and the aluminum alloy support frame. The readout side (top layer) of the PCB board integrates two key functional regions: the low voltage (LowV) region and the mesh voltage (MeshV) region. The LowV region serves primarily to extract residual charges from the non-functional readout region (copper-clad region), while the MeshV region is responsible for supplying the operating voltage to the Micromegas detector. The PCB bottom layer features dedicated pad interfaces that connect to an external power-supply board, providing regulated voltages and distributed power to the detector.

The feasibility study of TPC detector was initiated for the CEPC Technical Design Report (TDR). This study aims to identify feasible technical solutions and accumulate practical experience in the development of detector modules that satisfy the fundamental requirements of the CEPC detector concept design. The main objectives of this prototype are to set up and finalize the TPC module and the small prototype at the Institute of High Energy Physics, Chinese Academy Science.

Acknowledgments

This study was supported by the National Key Programme for *S&T* Research and Development (Grant NO.: 2024YFA1610600)

References

[1] K. Fujii et al., *ILC Study Questions for Snowmass 2021*, SLAC National Accelerator Lab., Menlo Park, CA, U.S.A. (2021) [arXiv:2007.03650].

[2] J. Gao, *CEPC Technical Design Report: Accelerator*, *Radiat. Detect. Technol. Methods* **8** (2024) 1 [arXiv:2312.14363].

[3] J. Kaminski, *TPC development by the LCTPC collaboration for the ILD detector at ILC*, *J. Phys. Conf. Ser.* **2374** (2022) 012149 [arXiv:2203.03435].

[4] W. Liu et al., *WASA: a low power and high integration readout ASIC for TPCs in 65 nm CMOS*, 2024 *JINST* **19** P04036.

[5] B. Qi et al., *Optimization of the double micro-mesh gaseous structure (DMM) for low ion-backflow applications*, *Nucl. Instrum. Meth. A* **976** (2020) 164282.

2026 JINST 21 C05004